sciendo

PRODUCTION ENGINEERING ARCHIVES 21 (2018) 20-23

PRODUCTION ENGINEERING ARCHIVES

ISSN 2353-5156 (print)
ISSN2353-7779 (online)

Exist since 4th quarter 2013
Available online at www.qpij.pl/production-engineering-archives

Bending fatigue strength coefficient the low carbon steel with impurities

Tomasz Lipiński[1]

[1] University of Warmia and Mazury in Olsztyn, The Faculty of Technical Sciences, Oczapowskiego 11 St., 10-957 Olsztyn, Poland, ORCID ID: 0000-0002-1644-1308, e-mail: tomasz.lipinski@uwm.edu.pl

Article history
Received 25.10.2018
Accepted 28.11.2019
Available online 31.01.2019

Keywords
steel
structural steel
non-metallic inclusions
oxide impurities
fatigue strength
bending fatigue

Abstract
The article discusses the results of a study investigating the effect of the number of fine non-metallic inclusions (up to 2 μm in size) on the fatigue strength of structural steel during rotary bending. The study was performed on 7 heats produced in an industrial plant. Fourteen heats were produced in a 100 ton oxygen converter. All heats were subjected to vacuum circulation degassing.
Steel sections with a diameter of 18 mm were hardened and tempered at a temperature of 200, 300, 400, 500 and 600°C. The experimental variants were compared in view of the applied melting technology and heat treatment options. The heat treatments were selected to produce heats with different microstructure of steel, from hard microstructure of tempered martensite, through sorbitol to the ductile microstructure of spheroidite. The results were presented graphically, and the fatigue strength of steel with a varied share of non-metallic inclusions was determined during rotary bending. The results revealed that fatigue strength is determined by the relative volume of fine non-metallic inclusions and tempering temperature.

DOI: 10.30657/pea.2018.21.04 JEL: L69, M11

1. Introduction

Steel is one of the most popular constructional material. The properties and practical applications of all constructional materials, including steel, are determined mostly by their microstructure. The parameters of high-grade carbon steels are influenced by a combination of factors, including chemical composition and production technology (Ulewicz, 2016; Mazur et al., 2016; Gerasin 2015; Selejdak et al., 2014).

The impurity content is also a key determinant of the quality of high-grade steel. Inclusions may also play an important role, dependent on their type and shape. The quantity and quality of non-metallic inclusions is determined mostly by the steel melting technology. Inclusions may increase the strength of steel by inhibiting the development of micro-cracks. One of the most popular crack prevention methods involves the formation of a material discontinuity at the end of the crack (e.g. an opening in organic glass). The quantity of non-metallic inclusions in steel is relatively low, nevertheless, they have a significant impact on the structure, technological and strength parameters of the resulting alloy. An effective method for the complete elimination of non-metallic inclusions has not been developed to date (Murakami 2002; Lipiński et al., 2015; Lis, 2002).

Although high quality low carbon steel has a relatively small number of non-metallic inclusions, those impurities have a considerable impact on the material's technological and strength parameters, in particular fatigue strength and life. Non-metallic inclusions play a special role in the process of steel hardening. Due to differences in the physical properties of steel and inclusion-forming phases, structural stresses are formed along inclusion boundaries (Cummings et al., 1957; Zhang et al., 2005, Lipiński et al., 2012).

Their negative impact on fatigue strength has been widely discussed in the literature (Beretta et al., 2001; Murakami 2002; Adamczyk et al., 2016), mostly in studies of hard-fatigue steels with low plasticity and inclusions larger than 5 μm. Selected authors have analyzed the purity and fatigue properties of steels with high plasticity. The effect of fine non-metallic inclusions measuring up to 5 μm on the fatigue strength of steel has not been thoroughly investigated. Hebsur observed that fatigue crack propagation decreased in steels where fine non-metallic inclusions were irregularly distributed (Hebsur et al., 1980). According to (Lipiński et al., 2015), steels produced with the use of various methods contain

mostly non-metallic inclusions of up to 2 μm in size. High-grade steel contains fewer large-sized inclusions. Non-metallic inclusions generally exert a negative effect of fatigue strength (Ulewicz et al., 2016; Lipiński, 2015, Drozin, 2016; Lenkovskiy et al., 2017). The above indicates that the dimensions of non-metallic inclusions significantly influence a material's fatigue strength.

The objective of this study was to determine the influence of fine non-metallic inclusions (up to 2 μm in size) on the fatigue strength of structural steel with high plasticity.

2. Materials and Methods

The experimental material consisted of steel products in an industrial plant. In the third process, steel was melted in a 100-ton oxygen converter and deoxidized by vacuum. Steel was cast continuously and square 100x100 mm billets were rolled with the use of conventional methods. Billet samples were collected to determine:

- chemical composition. The content of alloy constituents was estimated with the use of LECO analyzers, an AFL FICA 31000 quantometer and conventional analytical methods,
- relative volume of non-metallic inclusions with the use of the extraction method.

The number of particles range 2 μm and smaller was the difference between the number of all inclusions determined by chemical extraction and the number of inclusions measured by video method.

Analytical calculations were performed on the assumption that the quotient of the number of particles on the surface divided by the area of that surface was equal to the quotient of the number of particles in volume divided by that volume [20].

In aim of qualification of fatigue proprieties from every melting was tested 51 sections. The sections had the shapes of cylinder about 10 mm diameter. Their main axes were directed to direction of plastic processing simultaneously. The observations of microsections etched with nital revealed that steel tempering at various temperatures significantly affected the material's phase structure.It consisted in hardening from austenitizing by 30 minutes in temperature 880°C after which it was followed quenching in water, for which a drawing was applied . Tempering consisted in warming by 120 minutes material in temperature 200, 300, 400, 500 or 600°C and cooling down on air.

Fatigue strength was determined for all the heats. Heat treatment was applied to evaluate the effect of hardening on the fatigue properties of the analyzed material, depending on the volume of fine non-metallic inclusions. During a heat treatment, steel sections were hardened and tempered at a temperature of 200, 300, 400, 500 and 600°C. The application of various heat treatment parameters led to the formation of different microstructures responsible for steel hardness values ranging from 271 to 457 HV.

Examination was performed with the use of a rotatory curving machine with a frequency of pendulum cycles of about 6000 periods on minute. Fatigue defining endurance level of 10^7 cycles was accepted as its basis. The level of fatigue-inducing load was adapted to the strength properties of steel. Maximum load was set as follows:

- for steel tempered at a temperature of 200°C - 650 MPa,
- for steel tempered at a temperature from 300°C to 500°C - 600 MPa,
- for steel tempered at a temperature of 600°C - 540 MPa.

During the test, the applied load was gradually reduced in steps of 40 MPa (to support the determinations within the endurance limit). Load values were selected to produce 10^4-10^6 cycles characterizing endurance limits.

Coefficients *c* and *p* were substituted with coefficient *k* to convert equation (6) to (7).

$$k = \frac{z_g}{HV} \tag{1}$$

The significance of correlation coefficients r was determined on the basis of the critical value of the Student's t-distribution for a significance level α=0.05 and the number of degrees of freedom f = n-2 with formula (2).

$$t = \frac{r}{\sqrt{\frac{1-r^2}{n-2}}} \tag{2}$$

The average diameter of inclusion was calculated by means of the following formula:

$$d = \frac{\pi}{2}\left(\frac{\sum n_j}{\sum l_j^{-1}}\right) \tag{3}$$

where:
n_j – counts of inclusions,
l_j – average diameter of inclusions, μm

3. Results and discussions

The average chemical composition of the analyzed steel is presented in Table 1.

Table 1. average chemical composition of the analyzed steel

C	Mn	Si	P	S	Cr	Ni	Mo	Cu	B
0.24	1.17	0.24	0.018	0.016	0.52	0.52	0,24	0.02	0.003

Statistically significant the bending fatigue strength relationship of steel hardened and tempered at 200°C in dependence on the volume of impurities ranging up to 2 μm, is presented in Fig. 1, and regression equation with corre-lation coefficients r at (4), where d is average inclusion diameter.

$$k_{(200)}=1.5221d-1.3589 \text{ with } r=0.8865 \tag{4}$$

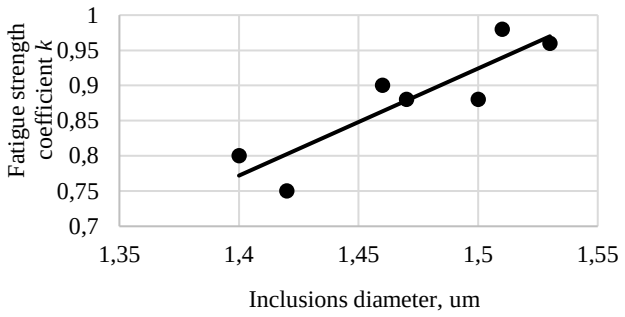

Fig. 1. Bending fatigue strength of steel hardened and tempered at 200°C subject to inclusions diameter k, µm

Statistically significant the bending fatigue strength relationship of steel hardened and tempered at 300°C in dependence on the volume of impurities ranging up to 2 µm, is presented in Fig. 2, and regression equation with corre-lation coefficients r at (5).

$$k_{(300)}=0.4706d+0.0134 \text{ with } r=0.7304 \quad (5)$$

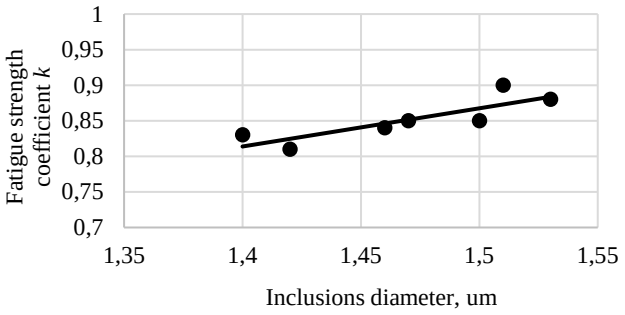

Fig. 2. Bending fatigue strength of steel hardened and tempered at 300°C subject to inclusions diameter k, µm

Statistically significant the bending fatigue strength relationship of steel hardened and tempered at 400°C in dependence on the volume of impurities ranging up to 2 µm, is presented in Fig. 3, and regression equation with corre-lation coefficients r at (6).

$$k_{(400)}=0.4706d+1.3568 \text{ with } r=0.6519 \quad (6)$$

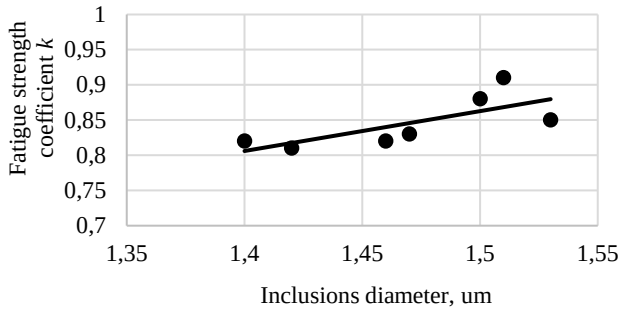

Fig. 3. Bending fatigue strength of steel hardened and tempered at 400°C subject to inclusions diameter k, µm

Statistically significant relationship bending fatigue strength of steel hardened and tempered at 500°C in dependence of volume the impurities range to 2 µm is presented in Fig. 4, regression equation and correlation coefficients r at (7).

$$k_{(500)}=05368d+0.0624 \text{ with } r=0.8451 \quad (7)$$

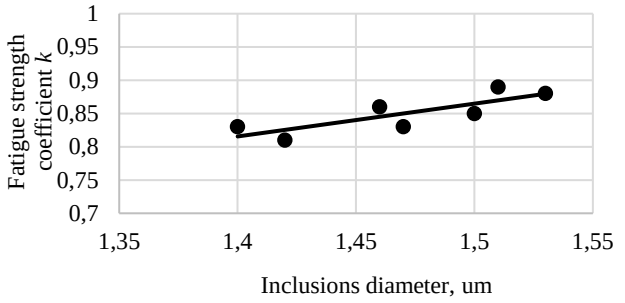

Fig. 4. Bending fatigue strength of steel hardened and tempered at 500°C subject to inclusions diameter k, µm

Statistically significant the bending fatigue strength relationship of steel hardened and tempered at 600°C in dependence on the volume of impurities ranging up to 2 µm, is presented in Fig. 5, and regression equation with corre-lation coefficients r at (8).

$$k_{(600)}=0.4926d+0.1258 \text{ with } r=0.8125 \quad (8)$$

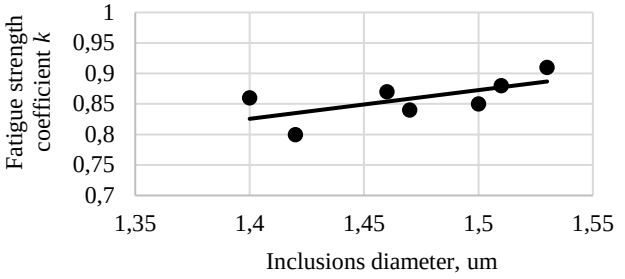

Fig. 5. Bending fatigue strength of steel hardened and tempered at 600°C subject to inclusions diameter k, µm

Statistically significant the bending fatigue strength relationship of steel hardened and tempered at all temperatures in de-pendence on the volume of impurities ranging up to 2 µm, is presented in Fig. 6, and regression equation with corre-lation coefficients r at (9).

$$k_{(200\text{-}600)}=0.7176d+0.1981 \text{ with } r=0.7046 \quad (9)$$

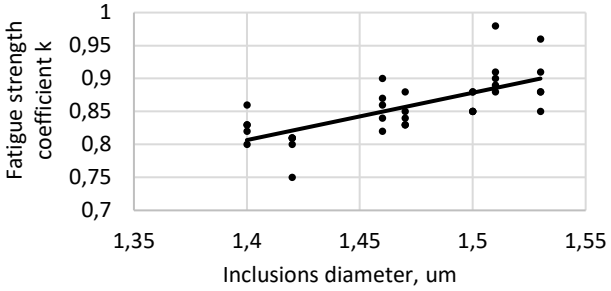

Fig. 6. Bending fatigue strength of steel hardened and tempered at all tested temperatures (200, 300, 400, 500 and 600°C) subject to inclusions diameter k, μm

The parameters representing correlation coefficients are present at Table 2.

Table 2. Parameters representing correlation coefficients

Tempering temperature °C	Correlation coefficient r	$t_{\alpha=0.05}$ calculated by (2)	$t_{\alpha=0.05}$ from Student's distribution for p=(n-2)
200	0.8865	8.3508	2.093
300	0.7304	4.6612	
400	0.6519	3.7472	
500	0.8451	6.8904	
600	0.8125	6.0752	
All	0.7046	4.3282	1.983

The regression equations, correlation coefficient r (3) – (9) was correlated with tempering temperature, correlation coefficient r. All regression equations were characterized by a high correlation coefficient of over 0.65, which points to high statistical significance confirmed by Student's t-test. The above data indicate that the equations describing parameter *k* at different tempering temperatures, where r=0.70, can be replaced with a single equation for all tempering temperatures (9).

4. Conclusion

1. This study demonstrated correlations between the diameter of impurities and the bending fatigue coefficient of non-metallic inclusions measuring at all range for high grade and high purity steels.
2. The proposed linear regression equations supported the determination of fatigue strength coefficient k and diameter of impurities with sufficient accuracy for every tempering temperature for high purity steels.
3. The influence of impurities on the fatigue strength coefficient of steel depends on its microstructure (tempered temperature).
4. With the decrease of plasticity of steel (matrix of impurities), the impact of diameter of impurities is more intense.

Reference

Adamczyk, M., Niżnik-Harańczyk, B., Pogorzałek, J., 2016. *Wpływ technologii wytapiania stali z dodatkiem stopowym 3÷5% al na rodzaj i morfologię wtrąceń niemetalicznych.* Prace Instytutu Metalurgii Żelaza, 2(68), 24-32 (In Polish).

Beretta, S., Murakami, Y., 2001. *Largest-Extreme-Value Distribution Analysis of Multiple Inclusion Types in Determining Steel Cleanliness.* Met. And Mat. Trans. B, 32B, 517-523.

Cummings, H.N., Stulen, F.B., Schulte,W.C., 1957. *Relation of inclusions to the fatigue properties of SAE 4340 steel*. Trans ASM, 49, 482-516.

Drozin, A.D., 2016. C*alculating of the True Sizes and the Numbers of Spherical Inclusions in Metal*. Metallography, Microstructure, and Analysis, 6(3), 240-246.

Gerasinm S, Kaliszm D., 2015. *Modeling of the Mn and S Microsegregation During Continuous Casting of Rail Steel.* Archives of Foundry Engineeringm 15(4), 35-38.

Lenkovskiym T.M., Kulyk V.V., Duriaginam Z.A., Kovalchukm R.A., Topilnytskyym V.H., Vira, V.V., Tepla, T.L., 2017, *Mode I and mode II fatigue crack growth resistance characteristics of high tempered 65G steel*. Archives of Materials Science and Engineering, 84(1), 34-41.

Lipiński, T., 2015. T*he influence of the distribution of nonmetallic inclusion on the fatigue strength coefficient of high purity steels.* Journal of Achievements of Materials and Manufacturing Engineering, 69(1), 18-25.

Lipiński, T., Wach, A., 2012. *The Effect of the Production Process and Heat Processing Parameters on the Fatigue Strength of High-Grade Medium-Carbon Steel*. Archives of Foundry Engineering, 12(2), 55-60.

Lipiński, T., Wach, A., 2015. *Dimensional structure of non-metallic inclusions in high-grade medium carbon steel melted in an electric furnace and subjected to desulfurization*. Solid State Phenomena, 223, 46-53.

Lis, T., 2002. *Modification of non-metallic dispersion phase in steel*. Met. and Foundry Eng. 1(28), 29-45.

Mazur, M., Mikova, K., 2016. *Impact Resistance of High Strength Steels.* Procidings Materialstoday 3(4), 1060-1063. https://doi.org/10.1016/j.matpr.2016.03.048

Murakami, Y., 2002. *Metal fatigue: Effects of small defects and inclusions*. Amsterdam Elsevier.

Selejdak, J., Ulewicz, R., Ingaldi, M. 2014. *The evaluation of the use of a device for producing metal elements applied in civil engineering.* 23rd International Conference on Metallurgy and Materials METAL, 1882-1888.

Ulewicz, R., 2016. *Influence of selected technological factors on fatigue strength*. Czasopismo Techniczne, Mechanika 3-M, 10, 9-14.

Ulewicz, R., Szataniak, P, 2016. *Fatigue Cracks of Strenx Steel.* Science Direct Materials Today: Proceedings, 3, 1195-1198.

Zhang, J.M., Zhanga, J.F., Yang, Z.G., Li, G.Y., Yao, G., Li, S.X., Hui, W.J., Weng, Y.Q. 2005.*Estimation of maximum inclusion size and fatigue strength in high-strength ADF1 steel*. Materials Science and Engineering A, 394.

弯曲疲劳强度系数低碳钢含杂质

關鍵詞
钢
结构钢
非金属夹杂物
氧化物杂质
疲劳强度
弯曲疲劳

摘要
本文讨论了非金属夹杂物对非金属夹杂物疲劳的影响。该研究是在工厂中产生的7次加热下进行的。在100吨氧气转换器中产生了14次加热。所有加热均进行真空循环脱气。
用直径为18毫米的钢板切片硬化并在200，300，400，500和600℃的温度下回火将实验变体与应用的熔化技术和热处理选项进行比较。选择热处理以产生回火马氏体的显微组织，通过回火马氏体的显微组织，通过山梨糖醇到球状体的韧性微观结构。结果以图形方式显示，并且非旋转弯曲的疲劳。结果再次证明了疲劳强度。